Effect of Silicone Dioxide and Poly(ethylene glycol) on the Conductivity and Relaxation Dynamics of Poly(ethylene oxide)–Silver Triflate Solid Polymer Electrolyte

Nirali Gondaliya,[1,2] D. K. Kanchan,[1] Poonam Sharma,[1] Prajakta Joge[1]

[1]*Physics Department, Faculty of Science, M. S. University of Baroda, Vadodara, Gujarat 390 002, India*
[2]*Department of Engineering Physics, Shri Sad Vidhya Mandal Institute of Technology, Bharuch, Gujarat, India*

Received 14 June 2011; accepted 29 September 2011
DOI 10.1002/app.36372
Published online 15 January 2012 in Wiley Online Library (wileyonlinelibrary.com).

ABSTRACT: The conducting and relaxation dynamics of Ag^+ ions in poly(ethylene oxide) (PEO)–silver triflate ($AgCF_3SO_3$) solid polymer electrolytes (SPEs) containing nanosize SiO_2 filler and poly(ethylene glycol) (PEG) as a plasticizer were studied in the frequency range 10 Hz to 10 MHz and in the temperature range 303–328 K. The comparatively lower conductivity of the plasticized (PEG) PEO–$AgCF_3SO_3$–SiO_2 nanocomposite electrolyte system was examined by analysis of the Fourier transform infrared (FTIR) spectroscopy and conductivity data. The electric modulus (M'') properties of the SPE systems were investigated. A shift of the M'' peak spectra with frequency was found to depend on the translation ion dynamics and the conductivity relaxation of the mobile ions. The value of the conductivity relaxation time was observed to be lower for the PEO–$AgCF_3SO_3$ system only with nanofiller SiO_2. The scaling behavior of the M'' spectra showed that the dynamical relaxation processes was temperature-independent in the PEO–$AgCF_3SO_3$ and PEO–$AgCF_3SO_3$–SiO_2–PEG polymer systems, whereas they were temperature-dependent for the PEO–$AgCF_3SO_3$–SiO_2 system. However, the relaxation processes of all of theses systems were found to be dependent on their respective compositions. © 2012 Wiley Periodicals, Inc. J Appl Polym Sci 125: 1513–1520, 2012

Key words: amorphous; composites; modulus; nanoparticle; relaxation

INTRODUCTION

The development of solid polymer electrolytes (SPEs) has drawn much interest from researchers.[1–3] High-molecular-weight poly(ethylene oxide) (PEO)-based composite polymer electrolytes have emerged as the best candidates for use as polymer matrices because of their solvation power, complexation ability, and ion-transport mechanisms directly connected with the alkaline cell. SPEs have many advantages, namely, a high ionic conductivity, high specific energy, wide electrochemical stability windows, light weight, and easy processability.[4] However, the low ionic conductivity of SPEs at ambient temperature limits their application.[5] Thus, considerable efforts have been devoted to improving the ionic conductivity of SPE. A common approach is the addition of nanosized fillers to the host polymer matrix; this has recently become an attractive approach because of the improved mechanical stability and enhanced ionic conductivity.[6–11] The fillers affect the PEO dipole orientation by their ability to align dipole moments, whereas the thermal history determines the flexibility of the polymer chains for ion migration. The approach generally improves the transport properties, resistance to crystallization, and stability of the electrode–electrolyte interface.[12] Another alternative approach is the addition of low-molecular-weight plasticizers to the nanocomposite polymer electrolyte system. Plasticization is the conventional way to reduce the crystallinity and increase the amorphous phase content of polymer electrolytes. Usually, both crystalline and amorphous phases are present in polymer electrolytes, but conductivity mainly occurs in the amorphous phase. The coupling between the polymer electrolytes is fascinating, and although it is not completely understood, it still holds the key to the development of new energy sources.[13]

From the physical point of view, the electrical modulus corresponds to the relaxation of the electric field in a material when the electric displacement remains constant.[14] It has been reported that the frequency-dependent conductivity and relaxation dynamics are both sensitive to the motion of charge species and dipoles of the polymer electrolytes.[15] For the close inspection of the relaxation dynamics, the

Correspondence to: D. K. Kanchan (d_k_kanchan@yahoo.com).

electric modulus (M'') formalism can be studied.[16] This modulus representation has been motivated by M'' displaying a peak and thereby associating a timescale [relaxation time (τ)] with the extent of conductivity. On the other hand, the modulus representation is still a matter of debate,[17] although the relations among the different quantities are well defined. The usefulness of modulus representation is to suppress the signal intensity associated with electrode polarization or to emphasize small features at high frequencies.[17] Thus, M'' spectra provide an opportunity to investigate the conductivity and its associated relaxation in ionic conductors and polymers.[18]

It is quite interesting to study the relaxation dynamics because of the combined effect of a ceramic filler and a plasticizer on PEO–$AgCF_3SO_3$ salt-based polymer electrolytes. To our knowledge, only very few reports are available in the literature that discuss the combined effect of a plasticizer and a ceramic filler. Therefore, in this work, we studied the effect of a nanofiller and plasticizer on the relaxation dynamics of Ag^+ ions in a PEO–$AgCF_3SO_3$ polymer electrolyte system in the light of modulus studies. Also, the interaction of the electrolyte systems {polymer–salt (PS; PEO–$AgCF_3SO_3$), polymer–salt–nanofiller (PSN; PEO–$AgCF_3SO_3$–SiO_2), and polymer–salt–nanofiller–plasticizer [PSNP; PEO–$AgCF_3SO_3$–SiO_2–poly(ethylene glycol) (PEG)]} was analyzed by FTIR spectroscopy.

EXPERIMENTAL

In the first step, we prepared polymer films by mixing proper weight percentages of PEO and various proportions of silver triflate $AgCF_3SO_3$ (weight percentages; PS system), using acetonitrile as a solvent. In the second step, various proportions of nanoporous filler SiO_2 were added to the aforementioned system, that is, PEO–$AgCF_3SO_3$–SiO_2 (weight percentage; PSN system), and in the final step, the plasticizer PEG was added in different quantities to the nanocomposite system that is, PEO–$AgCF_3SO_3$–SiO_2–PEG (weight percentage; PSNP system). The solutions thus obtained were stirred constantly for 48 h at room temperature. We carefully prevented any contamination with the external ambient environment by performing all of the preparation steps in a controlled environment. The homogenized and viscous solution was cast in polytetrafluoroethylene Petri dishes. Solvent evaporation was carried out in a closed apparatus for 24–30 h at room temperature. Homogeneous membranes having thicknesses ranging from 20 to 50 μm with good mechanical strengths were obtained.

For the impedance measurement, the circular polymer electrolyte film was sandwiched between two silver electrodes 1 cm in diameter under spring pressure. Impedance measurements were carried out with a Solartron 1260 impedance gain phase analyzer (Berkshire, UK) in the frequency range 10 Hz to 10 MHz. The cell temperature was controlled in the temperature range 303–328 K. Vibrational spectroscopy (IR) was carried out with a Jasco 4100 series FTIR spectrophotometer at wave numbers ranging from 500 to 4000 cm^{-1}.

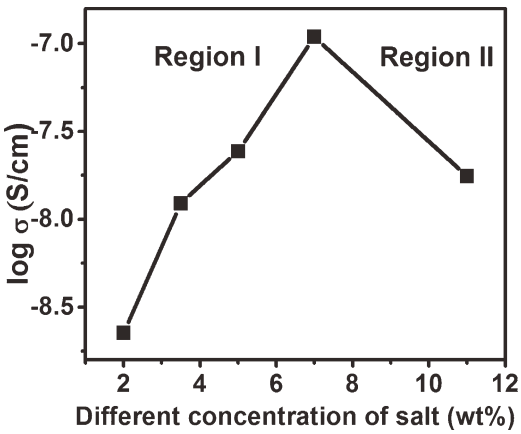

Figure 1 Plot of log σ versus different concentrations of $AgCF_3SO_3$ (wt %) in the PS system. σ = conductivity.

RESULTS AND DISCUSSION

Conductivity

Conductivity is an important factor to be considered in the production of better polymer electrolytes. Figure 1 shows the variation in the ionic conductivity with the addition of $AgCF_3SO_3$ salt. The composition of the highest conducting sample was observed to be PEO–7 wt % $AgCF_3SO_3$, and its conductivity at room temperature was 7.2329×10^{-7} S/cm. Further addition of salt (11 wt % $AgCF_3SO_3$) resulted in a sharp decrease in the conductivity values due to mechanical instability. From the conductivity studies, we observed that the conductivity value of the sample increased with increasing $AgCF_3SO_3$ concentration until it reached optimum value, and then, the conductivity decreased. These variations could be explained in terms of the number of free charge carriers or mobile ions. Therefore, region I, where the conductivity showed the increasing trend, was due to the dissociation of $AgCF_3SO_3$ salt producing more ions in the samples and resulting in an increase in the conductivity.[19] The decrease in the conductivity at concentrations greater than 7 wt % $AgCF_3SO_3$ (region II) may have been due to the higher rate of ion reassociation compared to the rate of ion dissociation,[1] or when ion dissociation dominated, too many ions were produced; this might have caused blocking of the conducting pathways.

Figure 2 shows the effect of SiO_2 nanofiller on the conductivity in the conducting PS sample. It was observed that the conductivity did not vary linearly

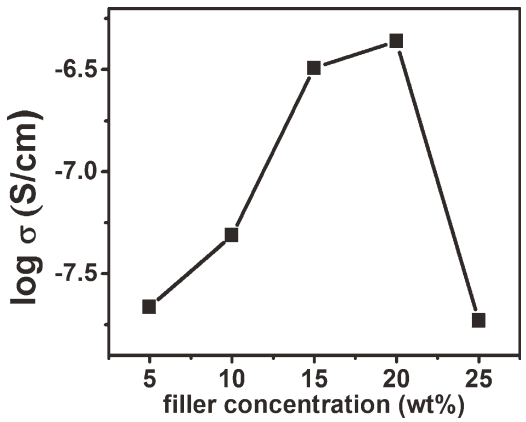

Figure 2 Plot of log σ versus different concentrations of the nanofiller SiO_2 (wt %) in the PSN system. σ = conductivity.

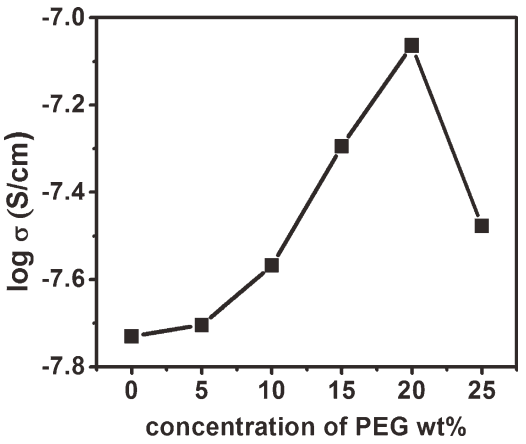

Figure 3 Plot of log σ versus different concentrations of the plasticizer PEG (wt %) in the PSNP system. σ = conductivity.

with the amount of the filler. Generally, ion movement is obstructed by the crystalline region present in composite polymer electrolytes by a blocking of the ion paths. The amorphous region, on the other hand, favored the conduction of Ag^+ ion because of its greater free volume. The addition of SiO_2 nanoparticles as a filler increased the ionic conductivity of the PSN composite polymer electrolytes through inhibition of the recrystallization of the PEO chains and by providing Ag^+ conducting pathways at the filler surface. According to the Lewis acid–base model,[20] the interaction among different species in a composite polymer electrolyte and nanofiller eases the conducting pathways to promote conduction. The incorporation of a nanofiller causes local PEO chain reorganization and leads to a high degree of disorder; this enhances the ionic conductivity.

The effect of the plasticizers on the polymer mobility and conductivity depends on the specific nature of the plasticizer, including its viscosity, dielectric constant, polymer–plasticizer interaction, and ion–plasticizer coordination. The effect of the plasticizers on the conformation and mobility of the host polymer depends on the plasticizer structure and the molecular weight, which influence the degree of mixing and the polymer–polymer or polymer–plasticizer interaction. Figure 3 shows the effect of PEG on the conductivity of the PSN sample. The plasticizer did not supply ions to the electrolyte system but helped to dissociate more salt into ions and had a low viscosity that could increase the ionic mobility. It was observed that the conductivity increased with up to 20 wt % PEG. This may have been due to the existence of separate ionic pathways for the migration of free Ag^+ ions through the plasticizer. The Ag^+ ions may have preferred to conduct through these new paths because the medium was less viscous, which enhanced the mobility of the ions. On the other hand, the plasticizer structure could influence the polymer plasticizer interactions by increasing interchain and intrachain separation and, hence, the free volume of the system. The decrease in the polymer–polymer interaction and the increase in the polymer–plasticizer interaction, in turn, influenced the glass-transition temperature (T_g) behavior.[21] However, a dilution effect predominated with further addition of the plasticizer to the system, and consequently, the conductivity dropped. This may have been due to the formation of linkages between the plasticizer itself, which caused it to recrystallize.

The impedance plots of the PS, PSN, and PSNP system at 303 K are shown in Figure 4. It is shown in the complex impedance plots that the semicircle of the PSN system shifted toward the origin, whereas that of the PSNP system shifted away from the origin, compared to the PS system. The second arc, which was observed only in the PSNP system, was due to the interfacial phenomenon on the

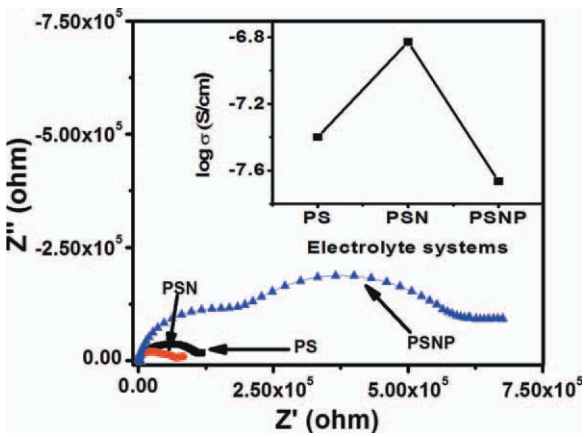

Figure 4 Plots of the impedance and log σ for different electrolyte systems: PS, PSN, and PSNP. σ = conductivity; Z' and Z'' = real and imaginary parts of complex impedance, respectively. [Color figure can be viewed in the online issue, which is available at wileyonlinelibrary.com.]

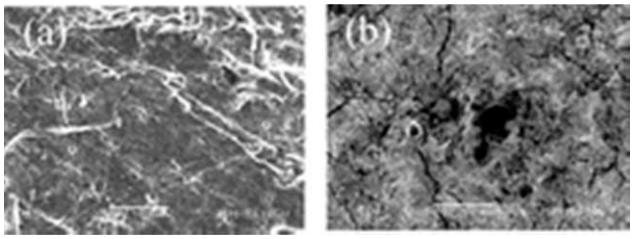

Figure 5 Scanning electron micrographs of the (a) PS and (b) PSNP electrolyte systems.

boundary of the polymer–silver electrode because of the presence of PEG. The bulk resistance of the PSN system compared to the PS system decreased, whereas for the PSNP system, the bulk resistance increased. This change in the bulk resistance is shown by the variation in the conductivity of these systems in the inset of Figure 4.

The decrease in the conductivity due to the addition of PEG in the PSNP system could be ascribed to the dielectric constant of the plasticizer, which played an important role in the modification of the conductivity of the polymer electrolytes.[22] It was reported[23] that the difference in the dielectric constant between PEO and PEG raised the possibility of chemical interaction; thus, the chemical bonds and linkages in the polymer complex were expected to be affected by the addition of the PEG plasticizer. PEO has strong solvating properties because of the high donating character of its numerous ether oxygens. The low dielectric constant arises from the high ratio of alkyl segments and a strong crystallization correlated with the high organization and rigidity of segmental units in PEO.[24] This crystallization is avoided by the addition of silver salt and nanofiller to inhibit regular packing and, thereby, modify the polymer structure to facilitate the conduction process. However, the addition of PEG must have promoted the organization of segmental units because of its similar nature to PEO. Consequently, the conductivity was observed to decrease with the addition of plasticizer (PEG) instead of increase.

Figure 5 shows the scanning electron micrographs of PSN and PSNP samples. It can be seen that the surface morphology of the PSN was a bit smooth and homogeneous. However, when the plasticizer PEG was added, the surface became uneven and rough.

FTIR spectroscopy

The FTIR spectra of the PEO, PS, PSN, and PSNP complexes are shown in Figure 6.

Pure PEO

For pure PEO, we observed the C—H stretching mode at 2876 cm^{-1}, CH_2 scissoring mode at 1466 cm^{-1}, CH_2 wagging mode at 1360 and 1341 cm^{-1}, CH_2 twisting mode at 1279 and 1241 cm^{-1}, and CH_2 rocking at 960 and 841 cm^{-1}. The semicrystalline phase of PEO was confirmed by the presence of the triplet peak of C—O—C stretching.[25,26] C—O—C stretching was found at 1145, 1095, and 1059 cm^{-1} vibrations, with the maximum intensity of the peak at 1095 cm^{-1}.

PEO–$AgCF_3SO_3$ (PS)

Suthanthiraraj et al.,[27] in their FTIR spectra of pure $AgCF_3SO_3$, reported that the peak at 634 cm^{-1} was due to δ_s (SO_3), and those at 1028 and 1112 cm^{-1} were due to γ_s (SO_3).[28,29] In this PS electrolyte system, the complexation of $AgCF_3SO_3$ with PEO was confirmed by the appearance of peaks at 638 and 1032 cm^{-1} belonging to δ_s (SO_3) and γ_s (SO_3) vibrations, respectively. Also, the shifting of peaks, which were observed in pure PEO, from 1457 to 1454, 2330 to 2335, 2360 to 2375, and 2877 to 2882 cm^{-1} was indicative of the complexation of the polymer PEO and $AgCF_3SO_3$.

PEO–$AgCF_3SO_3$–SiO_2 (PSN)

New peaks around 1646 and 1716 cm^{-1} were observed in the complexed (PS) PEO–$AgCF_3SO_3$ system after the addition of the SiO_2 nanofiller. The complexation between PEO–$AgCF_3SO_3$ and SiO_2 in the polymer matrix was proven by the change in intensity, the appearance of a new peak, changes in the existing peaks, and the broadening of the IR bands with the addition of SiO_2 in the polymer electrolytes; these also confirmed the increased amorphous nature of the sample.

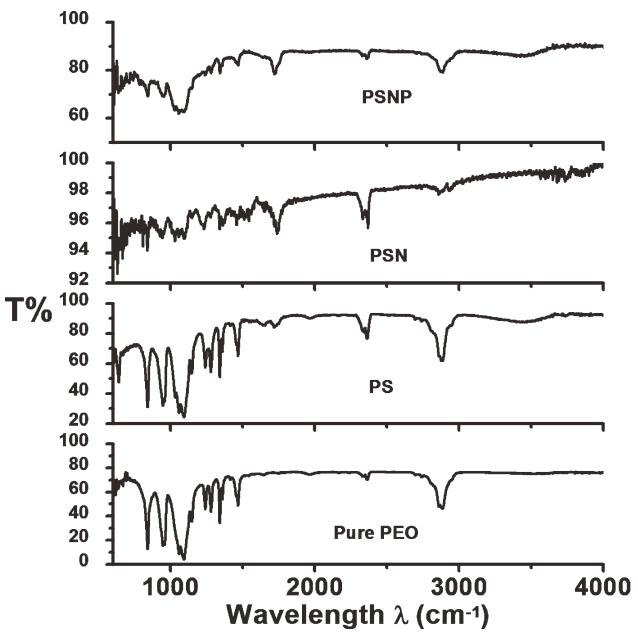

Figure 6 FTIR spectra of the pure PEO, PS, PSN, and PSNP electrolyte systems.

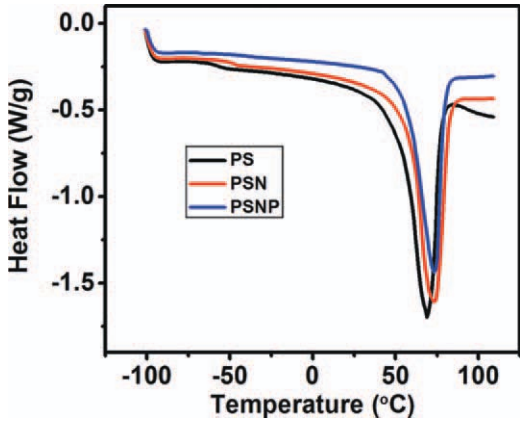

Figure 7 Differential scanning calorimetry curves of the PS, PSN, and PSNP systems. [Color figure can be viewed in the online issue, which is available at wileyonlinelibrary.com.]

PEO–$AgCF_3SO_3$–SiO_2–PEG (PSNP)

From the IR spectra (Fig. 6), it was quite evident that the intensities of the peaks at 1028, 1054, 1093, and 1146 cm^{-1} decreased and broadened. The addition of nanofiller increased the amorphous phase of the system and, thereby, decreased the intensity of the IR spectrum. However, with the addition of plasticizer (PEG) in the nanocomposite system, the peaks that were shouldered due to the incorporation of nanofiller reappeared; this indicated the degeneration of the amorphous phase in the system. This may have been due to the short branching or side-chain group of PEG, which produced a regular helical coil, which favored crystallization. The crystallization of polymer molecules into a crystalline lattice, that is, an organized structure, reduced the mobility and resulted in an increase in the rigidity and stiffness modulus.

Differential scanning calorimetry

The T_g and melting temperature (T_m) values of the PS, PSN, and PSNP systems were −59, −53.8, and −56.8°C and 68.9, 73.0, and 72.9°C, respectively. As depicted in Figure 7, the T_g value of the PSN system shifted toward the higher temperature side; this may have been due to the increase in the free volume with the incorporation of nanofiller, which resulted in an increase in the ionic mobility. With the addition of the plasticizer PEG, the glass transition shifted back to the lower temperature side; this may have been due to the linkage of PEO–PEG chains, which confirmed the segmental mobility of the chains or increased the crystalline content in the system. Similarly, T_m of the PSN system increased slightly compared to the PS system, but with the addition of PEG (in the PSNP system), no noticeable shift was observed.

Modulus

The dispersion behavior of the conductivity in the frequency domain is more conveniently interpreted in terms of the conductivity τ with the electrical modulus formalism. This is now widely used to analyze ionic conductivity by the association of the conductivity τ with the ionic process.

Figure 8(a–c) shows the imaginary part of the modulus of PEO–$AgCF_3SO_3$, PEO–$AgCF_3SO_3$–SiO_2 (PSN), and PEO–$AgCF_3SO_3$–SiO_2–PEG (PSNP) at different temperatures. The peak frequency range revealed the feature that all three systems were ionic conductors. This observed peak in all of the samples shifted toward the higher frequency side with increasing temperature. The frequency (f_{max}) of the modulus peak was assumed to represent a characteristic frequency of the conductivity relaxation. From Figure 8(a), it was clear that the M'' peak height nearly remained the same at all temperatures for the PS system. The constancy of the height of the modulus plots suggested the invariance of the dielectric constant and the distribution of τ with temperature.[30] In Figure 8(b), the peak height varies with temperature with the nanofiller, whereas in Figure 8(c), peaks with equal height were also observed when PEG was added.

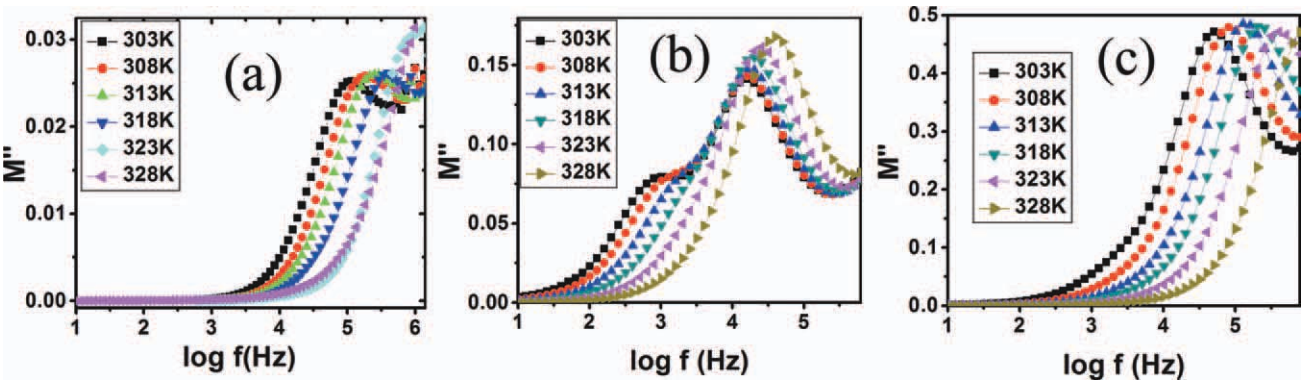

Figure 8 Imaginary part of the modulus versus the log frequency at different temperatures of (a) PS (7 wt %), (b) PSN (15 wt %), and (c) PSNP (20 wt %). [Color figure can be viewed in the online issue, which is available at wileyonlinelibrary.com.]

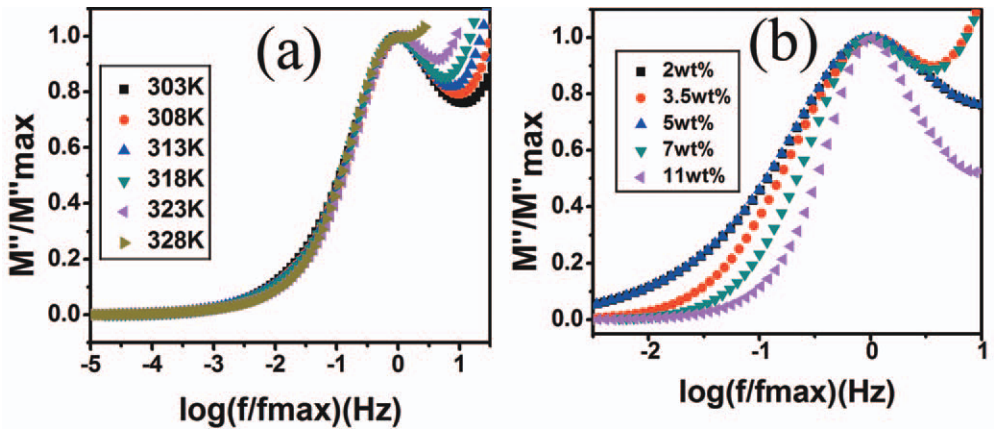

Figure 9 Normalized plot of M''/M''_{max} versus $\log(f/f_{max})$ for the (a) PS (5 wt %) system at different temperatures and (b) PS system at different salt compositions. [Color figure can be viewed in the online issue, which is available at wileyonlinelibrary.com.]

To observe the scaling behavior, we plotted the imaginary part of the dielectric modulus (M''/M''_{max}) as a function of the frequency $\log(f/f_{max})$ (where f is frequency) for PEO–$AgCF_3SO_3$ (PS) at different temperatures. From Figure 9(a), it is clear that the data points for the modulus plots coalesced very well for all temperatures, and the superimposition of plots indicated that the dynamical processes of ion transport were the same throughout the range of temperatures studied. The scaled spectra of M''/M''_{max} at different compositions for the PS system at 303 K are shown in Figure 9(b). The plot of M'' for all of the compositions exhibited different relaxation mechanisms. The nonmerging of the normalized plots indicated that the dynamical process of ion transport was not the same through the composition; in other words, the relaxation mechanism was composition-dependent.

A plot of M''/M''_{max} as a function of $\log(f/f_{max})$ for PSN at different temperatures is shown in Figure 10(a). It was observed that with the incorporation of the SiO_2 nanofillers, the data points in the modulus plots did not coalesce for temperature or different compositions of SiO_2, as shown in Figure 10(b). This indicated the different dynamical processes of ion transport.

However, in PSNP samples with the incorporation of plasticizer (PEG) in the PSN system, the data points for the modulus plots coalesced for all temperatures but did not coalesce for different compositions, as shown in Figure 11(a,b), respectively.

Figures 12 and 13 show the plots of the real and imaginary parts, respectively of the modulus versus log f for all three systems, namely, PS, PSN, and PSNP. The peak M''_{max} shifted toward the higher frequency side in PSN and PSNP with the addition of filler and plasticizer. The peak was assumed to be related to the translational ion dynamics and the conductivity relaxation of mobile ions. The shape of the spectrum was identical for all systems and showed a single relaxation peak. The observed long tail at low frequency was due to the large

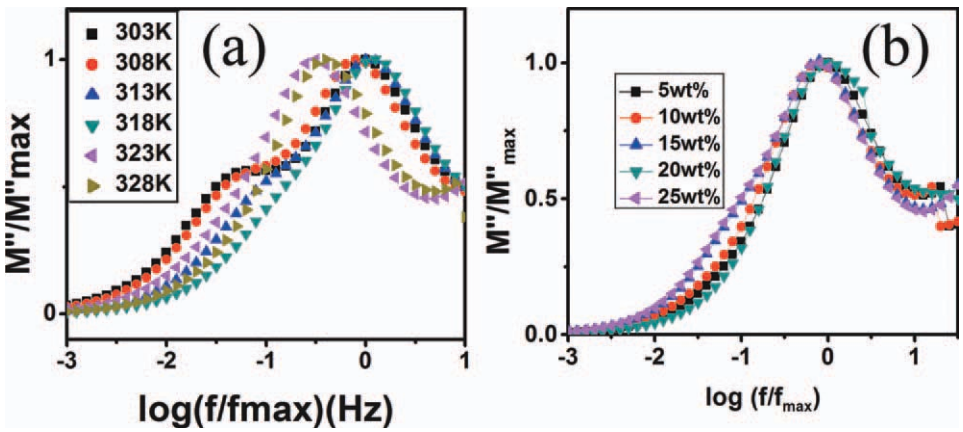

Figure 10 Normalized plot of M''/M''_{max} versus $\log(f/f_{max})$ for the (a) PSN (15 wt %) system at different temperatures and (b) PSN system at different compositions. [Color figure can be viewed in the online issue, which is available at wileyonlinelibrary.com.]

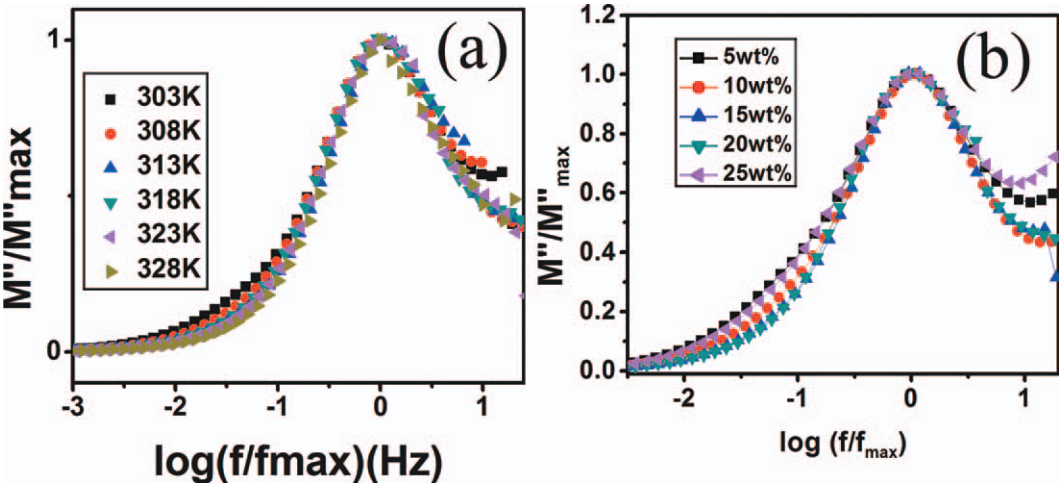

Figure 11 Normalized plot of M''/M''_{max} versus $\log(f/f_{max})$ for the (a) PSNP (20 wt %) system at different temperatures and (b) different PEG compositions in the PSNP system. [Color figure can be viewed in the online issue, which is available at wileyonlinelibrary.com.]

capacitance associated with the electrolytes. The broad and asymmetrical shape of M'' is generally described by the stretched exponential function of the electric field as follows:

$$\phi(t) = \exp[(-t/\tau)^{\beta}]$$

where ϕ is the stretched exponential function of the electric field, t is time, $0 \leq \beta \leq 1$ and β is the Kohlrausch exponent, respectively. The values of log τ for all three systems (PS, PSN, and PSNP) are given in Figure 14. It is shown in the figure that the conductivity τ decreased with the incorporation of the nanofiller. This indicated that the dispersion of nanosized filler strongly influenced the polymer backbone and immobilized it by repeatedly forming conducting pathways. These conducting pathways promoted the localized amorphous region. The increase in the amorphous region with the incorporation of filler was also evident from FTIR spectroscopy. This led to an increase in the ionic conductivity, as shown in Figure 4. However, with the addition of plasticizer (PEG) into the nanocomposite systems, τ was observed to increase. This was attributed to the suppression of the effect of the nanofiller with the addition of plasticizer. The addition of the plasticizer may not have been able to further reduce the recrystallization process, but it must have promoted it. Hence, a decrease in the ionic mobility with reduced ion transport was expected in the polymer electrolyte films.

CONCLUSIONS

The conductivity of pure PEO was enhanced by the addition of up to 7 wt % $AgCF_3SO_3$; more salt

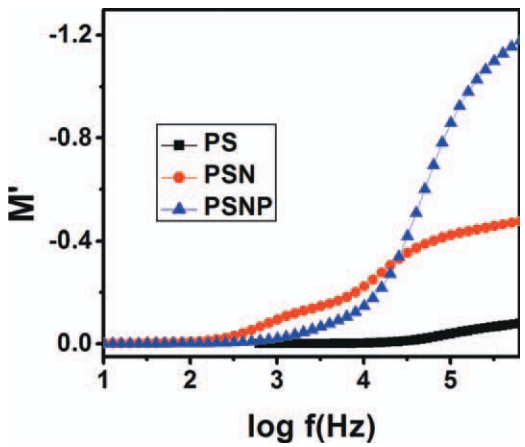

Figure 12 Real part of the modulus versus the log frequency for PS, PSN, and PSNP at room temperature. [Color figure can be viewed in the online issue, which is available at wileyonlinelibrary.com.]

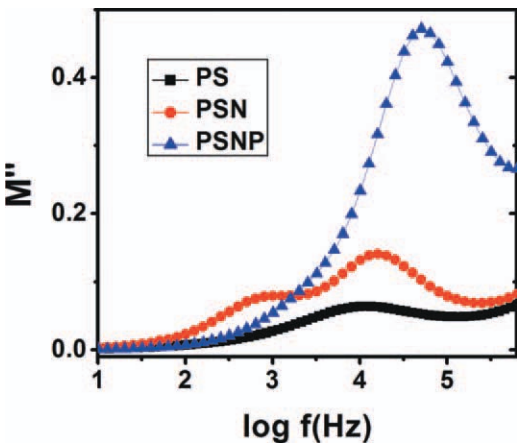

Figure 13 Imaginary part of the modulus versus the log frequency for PS, PSN, and PSNP at room temperature. [Color figure can be viewed in the online issue, which is available at wileyonlinelibrary.com.]

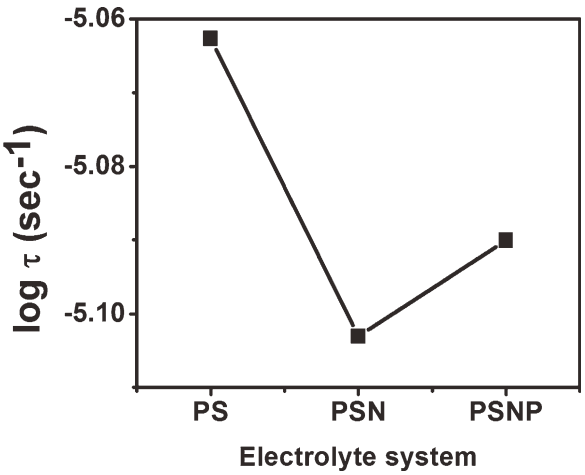

Figure 14 Variation of τ for the PS, PSN, and PSNP electrolyte systems.

resulted in diminished conductivity. A further enhancement in the conductivity was observed with the addition of the nanofiller SiO_2 to this PS system. However, the addition of the plasticizer PEG into this PSN composite electrolyte system resulted in a drop in the conductivity. The increase in the amorphous phase in the PEO electrolyte system having nanofillers resulted in the enhancement of the conductivity, whereas the reverse was observed with the decrease in the amorphous phase when the plasticizer PEG was added to this system. The addition of the plasticizer enhanced the recrystallization process in the nanocomposite system, which led to an increase in τ and, hence, a decrease in the mobility of the silver ions.

References

1. Teeters, D.; Robert, G. N.; Brian, D. T. Solid State Ionics 1996, 85, 239.
2. Sukeshini, A. M.; Kulkarni, A. R.; Sharma, A. Solid State Ionics 1998, 113–115, 179.
3. Pitawala, H. M. J. C.; Dissanayake, M. A. K. L.; Seneviratne, V. A. Solid State Ionics 2007, 178, 885.
4. Kim, J. Y.; Kim, S. H. Solid State Ionics 1999, 124, 91.
5. MacGlashan, G.; Andreev, Y. G.; Bruce, P. G. Nature 1999, 398, 792.
6. Wieczorek, W.; Stevens, J. R.; Florjanczyk, Z. Solid State Ionics 1996, 85, 67.
7. Croce, F.; Appetecchi, G. B.; Persie, L.; Scrosati, B. Nature 1998, 394, 456.
8. Quartarone, E.; Mustarelli, P.; Magistris, A. Solid State Ionics 1998, 110, 1.
9. Croce, F.; Curini, R.; Martinelli, A.; Persi, L.; Ronci, F.; Scrosati, B. J Phys Chem B 1999, 103, 10632.
10. Way, X. J.; Zhang, H. P.; Kang, J. J.; Wu, Y. P.; Fang, S. B. J Solid State Electrochem 2007, 11, 21.
11. Zhang, H.; Li, Z.; Wu, Y.; Wu, H. In New Trends in Ionic (Co) Polymers and Hybrids; Dragan, E. S., Ed.; Nova: New York, 2007.
12. Walls, H. J.; Zhou, J. U.; Yerian, J. A. J Power Sources 2000, 89, 156.
13. Natesan, B.; Karan, N. K.; Katiyar, R. S. Phys Rev E 2006, 48, 042801/1.
14. Molak, A.; Paluch, M.; Pawlus, S.; Klimontko, J.; Ujma, Z.; Gruszka, I. J Appl Phys D 2005, 38, 1450.
15. Singh, K. P.; Gupta, P. N. Eur Polym J 1998, 34, 1023.
16. Chabchoub, N.; Khemakem, H. J Alloys Compd 2004, 370, 8.
17. Richert, R. J Non-Crystalline Solids 2002, 305, 29.
18. Migahed, M. D.; Ishra, M.; Fahmy, T.; Barakat, A. J Phys Chem Solids 2004, 65, 1121.
19. Tan, C. G.; Siew, W. O.; Pang, W. L.; Osman, Z.; Chew, K. W. Ionics 2007, 13, 361.
20. Croce, F.; Persi, L.; Scrosati, B.; Serriano, F.; Plichta, E.; Hendrickson, M. A. Electrochim Acta 2001, 46, 2457.
21. Forsyth, M.; Meakin, P.; MacFarlane, D. R.; Hill, A. H. Electrochem Acta 1995, 40, 2349.
22. Haldar, B.; Singru, R. M.; Maurya, K. K.; Chandra, S. Phys Rev B 1996, 54, 7143.
23. Manoj, K.; Seknon, S. S. Ionics 2002, 8, 223.
24. Patrick, J.; Reichert, D.; de Azevedo, E. R.; Bonagamba, T. Acta Chim Slov 2005, 52, 349.
25. Rocco, A. M.; Fonseca, C. P.; Pereira, R. B. Polymer 2002, 43, 3601.
26. Tang, Z.; Wang, J.; Chen, Q.; He, W.; Shen, C.; Mao, X. X.; Zhang, J. Electrochim Acta 2007, 52, 6638.
27. Suthanthiraraj, S. A.; Joseph, P. B. Ionics 2007, 139, 365.
28. Huang, W.; Frech, R.; Wheeler, R. J Phys Chem 1994, 98, 100.
29. Deepa, M.; Sharma, N.; Agnihotry, S. A.; Chandra, R. J Mater Sci 2002, 37, 1759.
30. Reau, J. M.; Rossignol, S.; Tanguy, B.; Rojo, J. M.; Herrero, P.; Rojas, R. M.; Sans, J. Solid State Ionics 1994, 74, 65.